JFE TECHNICAL REPORT
No. 25 (Mar. 2020)

Evaluation Technology for Reliability of Equipment — Vibration Diagnosis —

NISHINA Yoshiaki[*1] ISHIGAKI Yusuke[*2] IMANISHI Daisuke[*3]

Abstract:

Recently, maintenance and renovation of aging equipment become a big issue in steelworks to improve the productivity and avoid fatal breakdown of production lines. JFE Group has successfully developed various new evaluation technologies for reliability of equipment that enable the group to assess and maintain equipment properly. They have greatly contributed to the steady delivery of the products, and high productivity of equipment in the steelworks. This paper introduces their typical example by vibration diagnosis.

1. Introduction

Because the Japanese steel industry constructed many facilities in the 1960s supported by internal and external demand accompanying high economic growth, much of that equipment is now showing deterioration with age. At JFE Steel as well, many facilities have been in service for more than 30 years since construction, and evaluation of equipment reliability has become a critical issue from the viewpoints of improving productivity and avoiding fatal breakdowns of production lines. In order to optimize the timing of equipment maintenance and renovation of aging equipment, the JFE Group has developed diagnostic technologies for quantitative evaluation of the reliability of various types of equipment.

As examples of the development of equipment reliability evaluation technologies employing vibration diagnosis, this paper introduces a vibration prevention countermeasure for maintaining high productivity in desulfurization equipment and a crack diagnosis technique for the crane runway girders by the Sonic-IR (vibro-thermography) crack diagnosis method.

2. Vibration Prevention of KR Desulfurization Equipment

In the mechanical stirring desulfurization process for molten iron using an impeller, strengthening stirring intensity in order to accelerate the reaction between the molten iron and the desulfurizing agent is important for shortening the treatment time and reducing unit consumption of the desulfurizing agent. Increasing the rotation speed of the impeller is an effective for strengthening stirring intensity, but when the impeller speed is increased, vibration of the equipment also increases, and this may lead to equipment trouble, depending on the degree of vibration. For this reason, placing a certain limit on the impeller speed was unavoidable.

At the Fukuyama 3KR (Kanbara Reactor) desulfurization equipment, the increase in equipment vibration became remarkable above a certain impeller speed, and high speed impeller rotation was impossible due to the high danger of equipment failure. Therefore, vibration countermeasures were studied based on an evaluation of the vibration characteristics of the actual equipment.

2.1 Outline of Fukuyama 3KR Desulfurization Equipment

Figure 1 shows the layout of the Fukuyama 3KR desulfurization equipment and the equipment arrangement. Although Fukuyama 3KR has three weighing

† Originally published in *JFE GIHO* No. 44 (Aug. 2019), p. 22–28


[*1] Senior Researcher Deputy General Manager,
Cyber-Physical System Research & Development Dept.,
Steel Res. Lab.,
JFE Steel


[*2] Senior Researcher Manager,
Cyber-Physical System Research & Development Dept.,
Steel Res. Lab.,
JFE Steel


[*3] Senior Researcher Deputy Manager,
Cyber-Physical System Research & Development Dept.,
Steel Res. Lab.,
JFE Steel

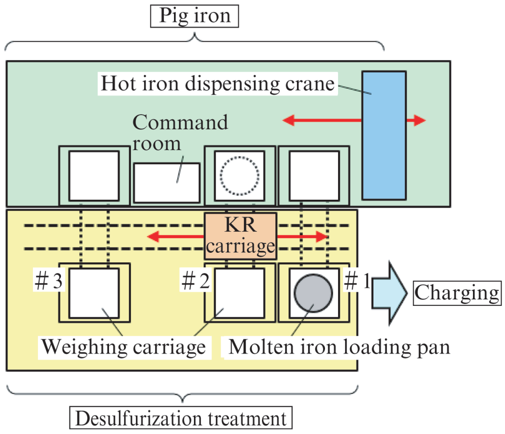

(1) Layout

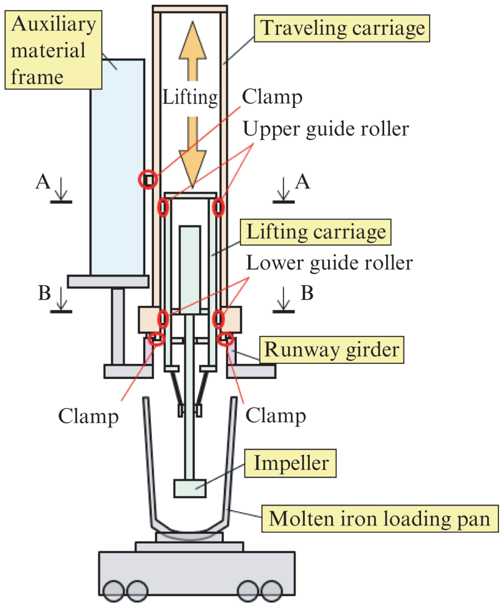

(2) Facility arrangement (side view)

Fig. 1 Outline of Fukuyama 3KR desulfurization facility

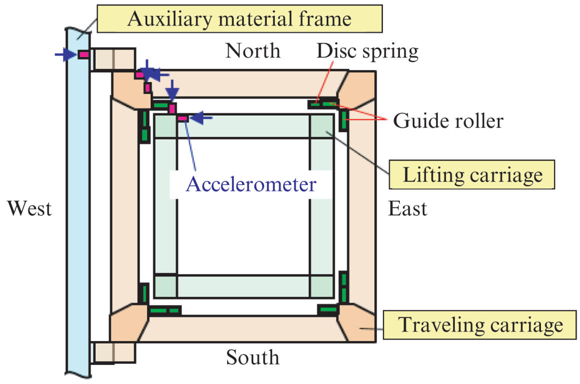

(1) Upper guide roller position cross-sectional view
(Fig.1 (2) A-A cross-sectional view)

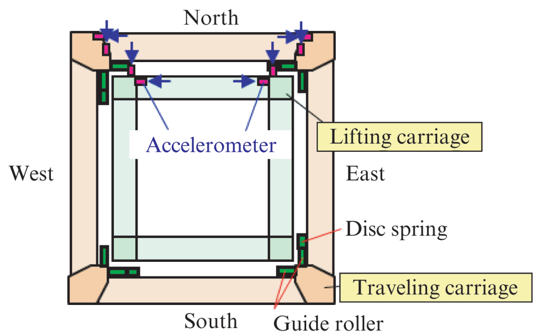

(2) Cross-sectional view of lower guide roller
(Fig.1 Cross-sectional view of (2) B-B)

Fig. 2 Accelerometer mounting position (13 points in total)

pits and carriages, it is possible to perform desulfurization treatment at the three locations with one impeller by moving the traveling carriage on the runway girder. The traveling carriage that moves on the runway girder is fixed to the runway girder and auxiliary material frame at the position of the molten iron loading pan, where desulfurization is performed. On the inner side of the traveling carriage, the lifting carriage is supported by guide rollers and disk springs, and the impeller is immersed in the molten iron and stirring is performed by lowering the lifting carriage itself.

2.2 Vibration Countermeasure

2.2.1 Vibration measurement of actual equipment

Vibration measurements using accelerometers were carried out to understand the condition of the vibration increase in the actual equipment. In these measurements, the impeller speed was changed in steps, and the molten iron was stirred while maintaining the rotational speed for 30 s under each condition. The accelerometer mounting positions are shown in **Fig. 2**. Here, the blue arrows show the measurement direction of each accelerometer. In order to measure the vibration of the traveling carriage, lifting carriage and auxiliary material frame, respectively, and to understand the movement of the traveling carriage and lifting carriage during these measurements, accelerometers were mounted so as to enable measurement of the vibration of two horizontal components (east-west direction and north-south direction) at the upper guide roller position and lower guide roller position.

Figure 3 shows the relationship between the impeller rotation speed and vibration acceleration obtained by the vibration measurements. The *x*-axis shows the normalized rotation speed, where 1 represents the rotation speed at which vibration which begins to exceed the allowable acceleration of the equipment. When the value on the *x*-axis exceeds 1, the vibration of the equipment as a whole increases by as much as 4 times, corresponding to the rotation speed. Based on this, it can be inferred that resonance of the equipment due to

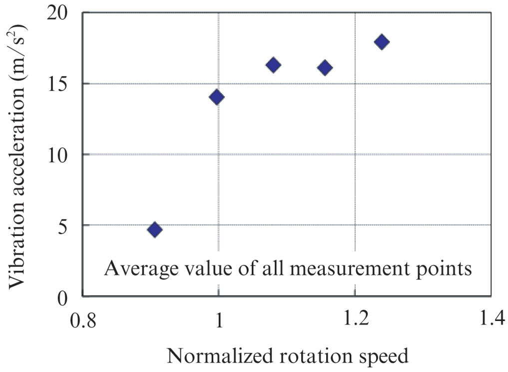

Fig. 3 Vibration measurement result of conventional impeller

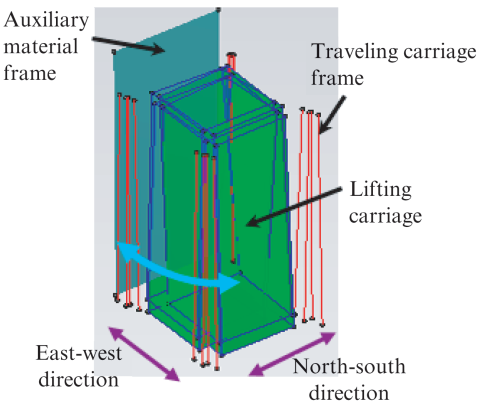

Fig. 4 Visualization of actual machine vibration

impeller rotation has occurred.

Figure 4 shows a visualization of the vibration for the condition when the normalized impeller rotation speed is 1. It can be understood that severe whirling of the traveling carriage and lifting carriage has occurred accompanying impeller rotation.

2.2.2 Evaluation of impeller vibration characteristics

A hammering vibration test was carried out to evaluate the vibration characteristics of the impeller. **Figure 5** shows the positions of the measurement point and the excitation point. The impeller was lowered to the treatment position without molten iron in the vessel, the flange parts were excited with an impact hammer in the north-south and east-west directions, respectively, and the generated vibration was measured.

Figure 6 shows the results of the frequency response obtained by the hammering vibration test. Here, peaks of the acceleration response, which indicate resonance, can be seen at 2.9 Hz and 8.6 Hz. An evaluation of the vibration mode by an experimental mode analysis revealed that these frequencies correspond to primary bending and secondary bending of the impeller. Since

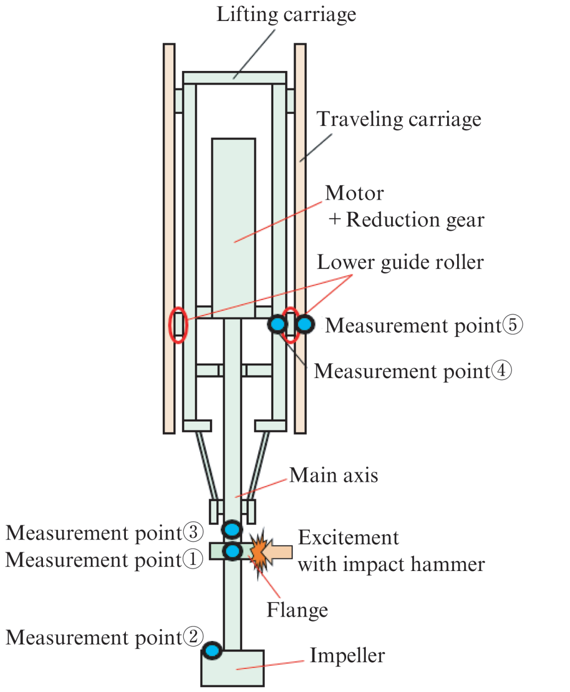

Fig. 5 Position of measurement point and excitation point

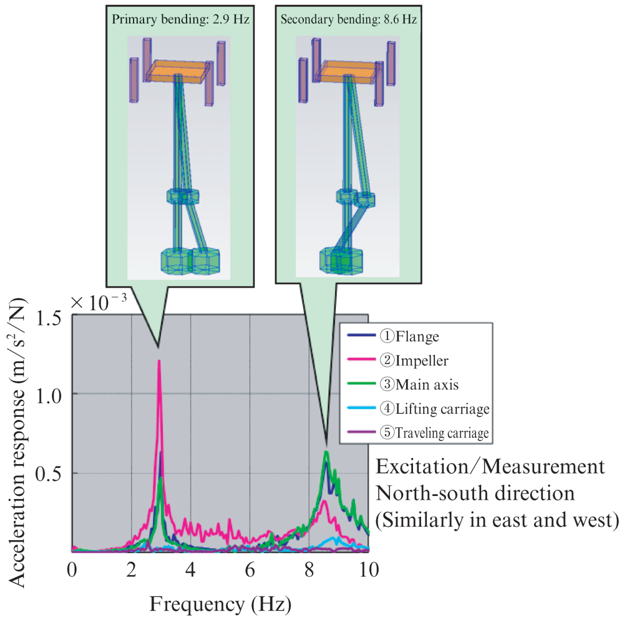

Fig. 6 Frequency response and vibration mode

the natural frequency of primary bending, i.e., 2.9 Hz, is also close to the natural frequency generated by the impeller, it is thought that the increase in vibration when impeller rotation was speeded up is caused by resonance of the primary bending vibration of the impeller. Therefore, separation of the natural frequency of primary bending vibration of the impeller from the natural frequency generated by impeller rotation can be considered an effective vibration countermeasure.

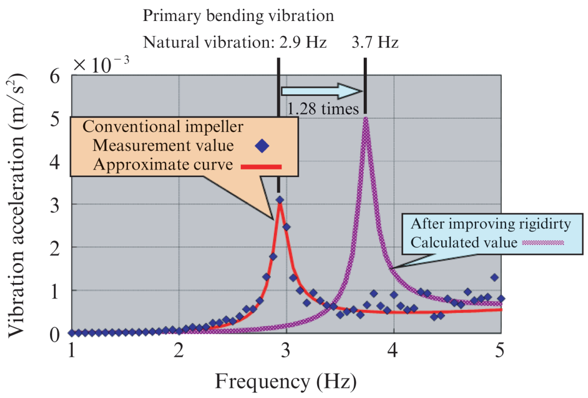

Fig. 7 Examination of vibration response characteristics of impeller

2.2.3 Vibration reduction by increasing impeller rigidity

Increasing the rigidity of the impeller was studied as a measure for preventing the vibration increase due to resonance of the impeller. Based on the results of the hammering vibration test of the impeller, the vibration response characteristics of the impeller were evaluated, taking into account the increase in centrifugal force due to impeller rotation. The results of this evaluation are shown in **Fig. 7**. Based on these results, a study was carried out with the target of holding vibration of the equipment to within the allowable range even in case of high speed impeller rotation. It was estimated that increased vibration due to resonance could be suppressed by increasing the conventional natural frequency of primary bending vibration of 2.9 Hz by 1.28 times, to 3.7 Hz, and as a result, a large decrease in vibration acceleration would be possible even under high speed impeller rotation.

Generally, the natural frequency f_n of the bending vibration of a beam can be expressed by the following equation.

$$f_n = \frac{\lambda_n^{\,2}}{2\pi L^2}\sqrt{\frac{EI}{\rho A}} \quad \cdots\cdots (1)$$

where, λ_n is a coefficient determined by the boundary condition, E is Young's modulus, I is the geometrical moment of inertia, ρ is density, A is the cross-sectional area of the beam and L is the length of the beam. Because bending vibration of an impeller can be regarded as bending vibration of a beam with one fixed end, the natural frequency of bending vibration of the impeller is proportional to the square root of the geometrical moment of inertia. Therefore, the natural frequency of primary bending vibration can be increased by 1.28 times by increasing the conventional geometrical moment of inertia of the impeller shaft by 1.63 times.

Table 1 Changing sectional shape of impeller

	Conventional impeller	Large diameter impeller
Cross-sectional shape	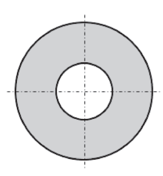	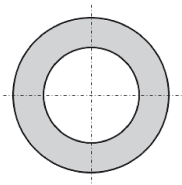
Outer diameter ratio	1	1.18
Thickness ratio	1	0.68
Cross-sectional area ratio = weight ratio	1	0.96
Section moment of inertia ratio	1	1.65
Natural frequency	2.9 Hz (Experimental value)	3.7 Hz (Calculated value)

Use of a large-diameter impeller shaft to increase the geometrical moment of inertia of the impeller shaft was studied. **Table 1** shows the cross-sectional shapes of the conventional impeller and the large-diameter impeller. Both have a hollow structure, but the geometrical moment of inertia of the large-diameter impeller was increased by increasing the outer diameter ratio of the shaft core to 1.18 times that of the conventional impeller. Since the natural frequency will decrease if the cross-sectional area is increased, a thin-wall design was adopted so that the cross-sectional area was equal to or less than that of the conventional impeller. As a result, the cross-sectional area was maintained while increasing the geometrical moment of inertia by 1.65 times, thereby increasing the natural frequency by 1.28 times. Thus, a decrease in vibration was expected by replacing the conventional impeller with the large-diameter impeller.

2.2.4 Verification of effect of large-diameter impeller

The vibration when stirring molten iron with the large-diameter impeller was measured in the same manner as the above-mentioned vibration measurements for the conventional impeller. **Figure 8** shows the relationship between the impeller rotation speed and vibration acceleration, together with the results for the conventional impeller. Here, the impeller rotation speed was normalized in the same way as in Fig. 3.

When using the conventional impeller, vibration increased rapidly as the rotation speed was increased from the low speed region. However, when the large-diameter impeller was used, the same level of vibration

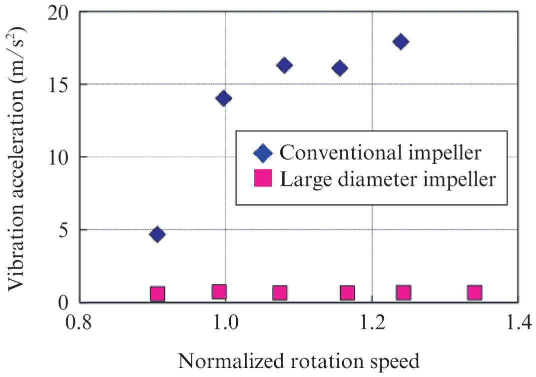

Fig. 8 Vibration measurement result of actual equipment (comparison between conventional impeller and large diameter impeller)

as in the low speed region could be maintained even during high speed rotation, showing that the large-diameter impeller could suppress the vibration increase caused by resonance. It may be noted that the vibration acceleration with the conventional impeller and the large-diameter impeller was different in the low speed region. However, this is thought to be due to differences in the condition of adhering metal or bending of the shaft core due to the timing of measurement.

As a result of the development described above, resonance due to impeller shaft rotation was avoided and a decrease in equipment vibration could be realized by adopting a large-diameter impeller to increase impeller rigidity.

2.3 Summary

A countermeasure for vibration of the Fukuyama 3KR desulfurization equipment was implemented in order to achieve higher refining efficiency by high speed rotation of the impeller. The following conclusions were obtained.

(1) An evaluation of the vibration characteristics of the impeller revealed that the natural frequency of the primary bending vibration of the impeller was 2.9 Hz.

(2) This study clarified the fact that resonance of impeller bending vibration can be suppressed and high speed impeller rotations is possible by increasing the outer diameter of the impeller core.

3. Sonic-IR Crack Diagnosis Technology

A large number of large-scale overhead traveling cranes are used at steel works production lines for transportation of molten steel, steel slabs, product coils, etc. **Figure 9** shows the equipment composition of a general overhead traveling crane. An overhead traveling crane comprises traveling girders called runway girders, which are installed along the two walls of the building, a crane girder and a crab trolley. The

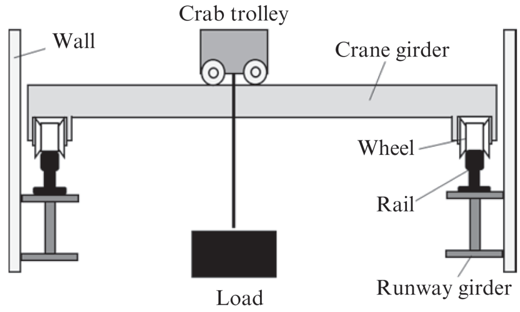

Fig. 9 Schematic illustration of overhead traveling crane

crane girder travels on the runway girders, and the crab trolley transports the object loads by hoisting and lowering.

Because overhead traveling cranes are frequently used for long periods of time once installed, and the weight of the loads being transported and the self-weight of the crane girder act on the runway girders as cyclical loads, many cases of fatigue damage have been reported[1]. Planned crack inspections and maintenance of the runway girders of overhead traveling cranes are conducted in order to prevent damage, as runway girder damage can lead to major accidents, including accidents involving death and injury, and also has a large effect on production lines. The crack inspection methods for runway girders include visual inspection from the ground and walkway on the crane, and ultrasonic testing (UT), magnetic particle testing (MT) and penetrant testing (PT) by assembling scaffolding. In visual inspections, it is extremely difficult to discover cracks on runway girders due to the adhering dust and dirt caused by long-term use. In the UT, MT and PT methods, the inspection device must be placed in direct contact with the object of inspection. However, runway girders are generally installed in high places, and inspection scaffolding must be set up to use these methods, resulting in poor inspection efficiency and high inspection costs. Therefore, this paper presents the results of a study of application of the Sonic-IR method[2–4] (also called the vibro-thermography method), which is one technique for detection of structural deterioration by infrared thermography, to remote, high efficiency inspection of fatigue cracks that occur in the runway girders of overhead traveling cranes in steel works in order to solve these problems.

3.1 Principle

Infrared (IR) thermography is now used in diverse fields, taking advantage of improvements in the resolution of temperature detection devices and performance of computers. In particular, infrared thermography has attracted attention as a high efficiency inspection technique in the field of nondestructive inspection (NDI)

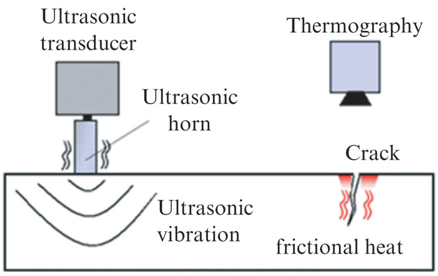

Fig. 10 Schematic illustration of principle of Sonic-IR method

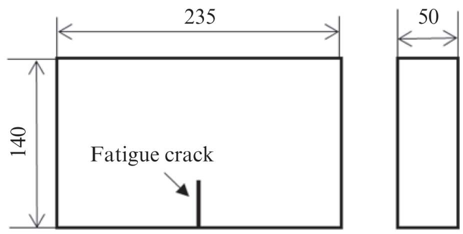

Fig. 11 Plate specimen shape and position of fatigue crack

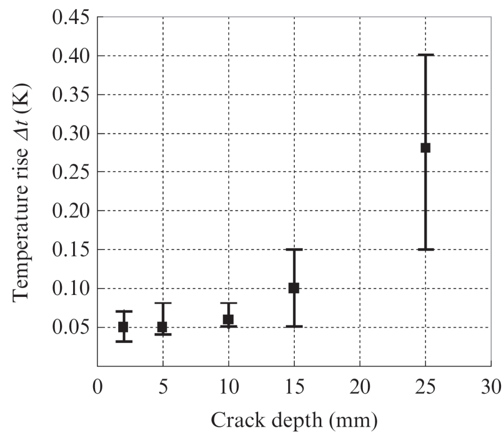

Fig. 12 Relationship between crack depth and temperature rise

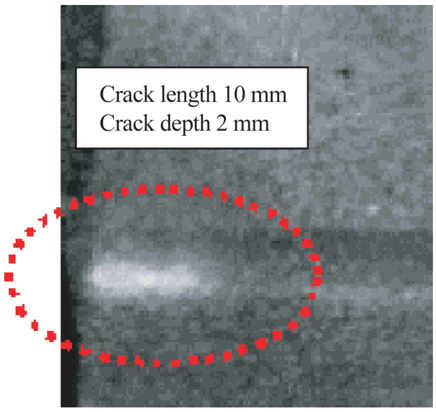

Fig. 13 Infrared image of the crack

as noncontact, remote measurement is possible and large surface areas can be measured. Among IR thermography methods, Sonic-IR is a crack inspection technique that employs a combination of IR thermography and an ultrasonic vibration generator. A model of the measurement principle is shown in **Fig. 10**. When a structure that contains a crack is excited continuously with large amplitude ultrasonic vibration, a local temperature rise occurs at the cracked part due to the action of friction and impact of the crack surfaces under compressive stress. This temperature rise is measured by IR thermography, and the crack is detected as a high temperature part. Since this technique uses the temperature rise due to friction and impact of the crack surfaces, it is applied to detection of closed cracks, which are considered difficult to detect by other crack inspection techniques. In particular, this technique is effective in detection of fatigue cracks, as many cracks caused by fatigue are closed cracks that are difficult to detect by visual inspection.

3.2 Result of Laboratory Study

3.2.1 Composition of experimental device

In this study, an ultrasonic welder (Kaijo Corporation, C-6281A) was used as the vibration generator. In ultrasonic welders, the vibration generated by the transducer is amplified by an ultrasonic horn made of SUS304 stainless steel, and the vibration is introduced into the object by placing the horn in contact with the object. In this study, the frequency and amplitude of the incident ultrasonic vibration were set to 19.5 kHz and 20 μm, respectively. The temperature distribution around the crack when vibration was introduced was measured by using an infrared thermography system (Cedip Infrared Systems, Jade III). In this test, InSb was used in the detection element of the infrared thermography system, providing temperature resolution of 0.02 K, and lock-in processing[5] was performed in the test to enhance crack detection accuracy. This technique improves the S/N ratio by taking the correlation of the measured time-series data with a reference signal for temperature fluctuation. The reference signal used here was the change over time in temperature rise at the connection between the ultrasonic vibration generator and the inspection object.

3.2.2 Evaluation of minimum crack depth detection performance

As shown in **Fig. 11**, the minimum crack detection depth of this technique was obtained by using samples in which fatigue cracks with depths from 2 mm to 25 mm were introduced in flat plates with dimensions of 140 mm × 235 mm × 50 mm. The results are shown in **Fig. 12**. The temperature increases as the crack depth becomes larger. **Figure 13** shows an infrared image of a crack with a depth of 2 mm and length of 10 mm,

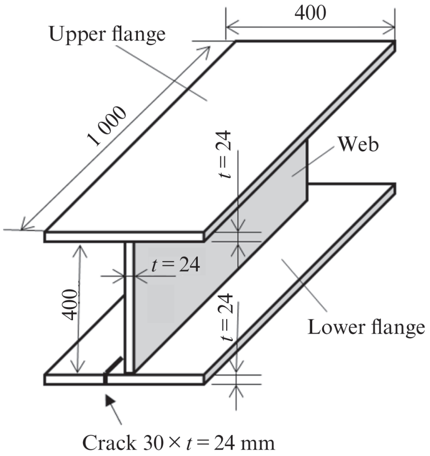

Fig. 14 Runway girder specimen shape and position of fatigue crack (Unit: mm)

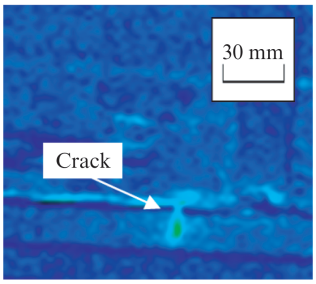

Fig. 15 Infrared image of the crack (Measured distance = 10 m)

which was the smallest size measured in this test. Detection of the crack with a depth of 2 mm was amply possible, as the average temperature rise in this case was approximately 0.05 K. In this experiment, the minimum detection target for cracks in runway girders was set at a crack depth of 24 mm based on an analysis of crack growth. Thus, this result showed that this target is achievable by the Sonic-IR technique, provided adequate vibration transmission is possible.

3.2.3 Verification of crack detectability

To study the detection distance limit of cracks in runway girders (in other words, the possible vibration transmission distance), a basic study was carried out using a SS400 specimen simulating a runway girder. The specimen geometry is shown in **Fig. 14**. Since the vibration transmission distance and existence of weld lines generally cause attenuation of ultrasonic vibration, the influence of attenuation in crane runway girders must be investigated when considering practical application. Therefore, this specimen was fabricated using a welded structure similar to that in actual crane runway girders, and a closed crack (depth: 24 mm, length: 30 mm) simulating a fatigue crack was introduced in the lower flange. In this test, vibration was induced in the upper flange, and the temperature distribution was measured by IR thermography. Two types of IR cameras were used, one with a normal lens having a focal distance of 50 mm, and the other with a telephoto lens having a focal distance of 200 mm.

Figure 15 shows an infrared image taken from a measurement distance of 10 m. The temperature rise was sufficient for crack detection, demonstrating that vibration introduced from the upper flange can be transmitted through the weld lines in the web part to a crack in the lower flange. This means that it is possible to detect cracks in the lower flange and web parts of actual runway girders by placing the vibration generator on the top flange, which is easily accessible from the walkway.

Next, the possibility of crack detection by IR thermography from different measurement distances was studied. As the distance between the IR thermography device and the object of measurement increases, the unit size per pixel (i.e., pixel resolution) also increases. Since the detectable crack size is closely related to pixel resolution, in theory, crack detection performance decreases as the measurement distance becomes longer. **Table 2** shows the possibility of crack detection at various measurement distances. As shown in this table, adequate detection of the standard-size crack (depth: 24 mm) is possible from a distance of 10 m if a telephoto lens is used. Because the height of many runway girders of overhead traveling cranes installed in steel works is no more than 10 m from the ground, remote detection of cracks in runway girders is possible by setting up the infrared thermography device on the ground.

Table 2 Result of remote crack detection (Crack depth: 24 mm)

	Measured distance (m)				
	1	5	10	15	20
Normal lens (Focal distance = 50 mm)	○	○	×	×	×
Telephoto lens (Focal distance = 200 mm)	○	○	○	○	×

○Detectable; ×Non-detectable

3.2.4 Verification of vibration transmission by vibration measurement

The vibration in the vicinity of the crack during excitation of the specimen simulating a crane runway girder was measured by using a laser type vibrometer (Keyence Corporation, LKG-15). **Figure 16** shows the results when the frequency component of the vibration frequency (19.5 kHz) was extracted and the relationship between its amplitude and the temperature rise due to heat generation by the crack was investigated. The open circles (○) indicate cases in which detection

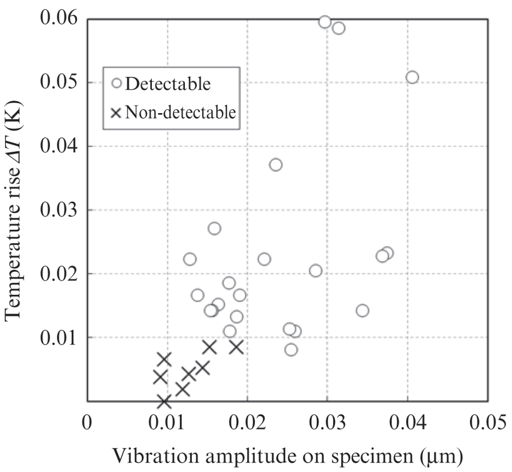

Fig. 16 Relationship between vibration amplitude and temperature rise

by the IR thermography device was possible, and the × marks indicate cases in which detection was not possible. When the vibration amplitude exceeded a threshold value of 0.02 μm, all cracks could be detected, showing that adequate vibration for heat generation reached the cracks. However, in applying Sonic-IR to crack detection of runway girders, it is assumed that efficient introduction of vibration will not be possible in some cases, for example, due to poor contact between the ultrasonic horn and the vibration surface or the shape or condition of the surface. Because cracks will not generate heat under such conditions, it goes without saying that the cracks cannot be detected. However, by simultaneously checking vibration transmission, it is possible to take appropriate action for poor transmission by cleaning the vibration surface, changing the excitation position, etc. By taking these measures, omissions in crack detection can be prevented, and inspection accuracy can be improved.

3.3 Summary

This paper described the results of a laboratory study of application of Sonic-IR, which is a technique using infrared thermography, to high efficiency, remote crack inspection of the runway girders of overhead traveling cranes. It was found that detection of the minimum size target crack derived by a crack growth analysis is amply possible by placing the vibration generator on the easily-accessible upper flange and setting up the infrared thermography device on the ground. The necessary vibration amplitude for crack detection was also clarified, and a system that prevents omissions in crack detection due to poor vibration transmission was developed.

4. Conclusion

As examples of the development of reliability evaluation technologies for equipment by vibration diagnosis, this paper introduced a countermeasure for vibration prevention with the aim of improving the productivity of desulfurization equipment, and a crack detection technique for crane runway girders by the Sonic-IR (vibro-thermography) diagnosis method. JFE Steel is working to improve productivity and avoid fatal equipment breakdowns at production lines by effectively utilizing these developed technologies.

References

1) Kiuchi, Y.; Maeda, Y. Survey of Degradation for Overhead Travelling Cranes. NIIS-SRR. 1996, no. 15, p. 7–15.
2) Henneke II, E.G.; Reifsnider, K.L.; Stinchcomb, W.W. Thermography — An NDI method for damage detection. J. Metal. 1979, vol. 31, p. 11–15.
3) Favro, L.D.; Han, Xiaoyan.; Ouyang, Zhong.; Sun, Gang.; Sui, Hua.; Thomas, R.L. Infrared imaging of defects heated by a sonic pulse. Review of Scientific Instruments.2000, vol. 71, p. 2418–2421.
4) Kawashima, K.; Murase, M.; Sukigara, N.; Tamayama, T; Okumura, T.; Yasui, M. Detection of tight cracks with thermos-sonic method. Journal of the Japan Society of Mechanical Engineers. 2004, p. 93–94.
5) Sakagami, T.; Nishimura, T.; Kubo, S. Development of self-reference look-in thermography and its application to crack monitoring. The 3rd Symposium on Evaluation and Diagnosis. 2004, no. 3, p. 123–127.